PERFORMANCES OF AN ARGON ARC-JET THRUSTER FOR SATELLITES

A. KAMINSKA[1], A. BIALEK[1], M. DUDECK[2]

[1]IEPE, Poznan University of Technology, ul. Piotrowo3a, Poznan 60-965, Poland
E-mail: aniela.kaminska@put.poznan.pl
[2]UPMC Univ. Paris 6, UMR 7190, Institut Jean Le Rond d'Alembert, F-75005 Paris, France
UPMC CNRS, UMR 7190, Institut Jean Le Rond d'Alembert, F-75005 Paris, France
E-mail: michel.dudeck@upmc.fr

Received July 24, 2014

Arc-jet thrusters are currently used for the propulsion of satellites. Low power arc-jet are functioning with propellant as helium, hydrogen, ammonia, lithium and argon. The performances such as axial thrust and specific impulse of a D.C. argon arc–jet are calculated by a fluid description of the arc with two kinetic temperatures (T_e,T) and non equilibrium condition for the ionization. The electric input power is calculated from the conductivity which is deduced from plasma properties. The influence of different angles of the nozzle divergent part, arc current and mass flow rates on arc-jet performances is discussed. It is shown that the thrust is 0.3-2.5 N and the specific impulse 80-210 s for an argon mass flow rate 0.4-1.2 g/s and a arc current of 40-120 A.

Key words: Arc-jet, space propulsion, plasma flow modeling

1. INTRODUCTION

Low power *direct current* (D.C.) arc plasma sources are studied and used for technical applications for industry and research, and for planetary applications in a broad range of power and with various propellants.

Many electric propulsion systems are currently proposed for spacecrafts as Hall effect thruster, gridded ion thruster, plasma pulsed thruster, field electron emission plasma source, micro-wave source, and arc-jet [1-3]. The choice of a propulsion system depends on the mission and performances of the available thrusters. For the change of trajectory from an elliptic (LEO) to a geostationary (GEO) orbit, the needed thrust is around 400 N and for the station-keeping of a geostationary satellite space the thrust is 80-100 mN. Propulsion systems are necessary to maintain the geostationary satellite (GEO) at its working orbit location because of gravitational perturbation effects (lunar and sun effects), solar wind and radiative solar pressure. This station-keeping is currently performed by Hall effect thruster (named HET, SPT or PPS), gridded ion thrusters (named GIT or GIS), or arc-jet thrusters (AJT). For a precise positioning for scientific mission, the required

thrust is 1-10 mN. For long interplanetary missions, the thrust has to be higher in order to minimize the time of the journey, and today this level of thrust is not accessible by electric thrusters. However, a Hall effect thruster has been successfully tested to reach a lunar orbit (with a PPS1350-G thruster from Snecma-SAFRAN Group/ France) for the ESA Smart1 mission, 2003-2004) [4, 5]. Electric thrusters are now proposed for nanosatellites for deorbitation, rendezvous or attitude control for scientific missions [6, 7]. The axial thrust of D.C. arc-jets is in the range 50 mN – 500 N for a specific impulse between 350 s and 1500 s. Arc-jet are also used for the simulation of the non-equilibrium plasma flows around a spacecraft during the cross of a planetary atmosphere for the analysis of the radiative energy fluxes toward the surface of a spacecraft and to optimize the thermal protections.

An arc-jet running with argon as propellant has been previously studied using a fluid, stationary, and axisymmetric description without turbulence effects. The plasma properties has been obtained with two kinetic temperatures, one common temperature T for heavy particles (neutral species and ions) and an electron temperature T_e [8, 9].

2. PLASMA SOURCE

The studied arc-jet thruster is an axisymmetric plasma source with a cylindrical throat where the arc is sustained and a conical divergent (figure 1). The throat and the divergent are made of copper. The arc is sustained between a small plane disk of 2 mm in diameter, made of thoriated (3%) tungsten and the surface of the throat (anode). The diameter and length of cylindrical throat is 4 mm. The length of divergent part of the nozzle is 55 mm and the nominal half angle is 30°.

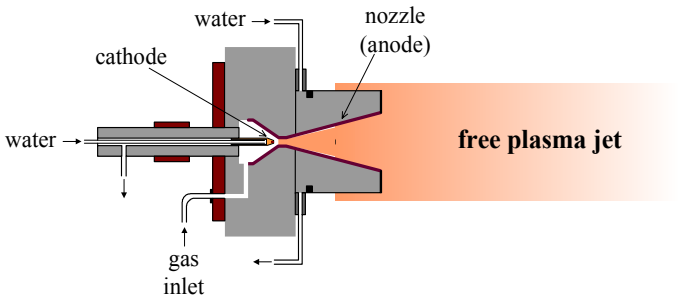

Fig. 1 – Schematic view of the arc-jet thrusters.

The arc-jet operates with the argon mass flow rate in the range of 0.1–1.3 g/s, the arc current from 60 to 140 A and the input electric power up to 4 kW.

3. MODEL

A detailed analysis of the plasma flow has been presented in [8, 9]. This flow is described solving stationary equations at the throat and the divergent part of the nozzle:

Electron Conservation: $$\nabla \cdot (n_e v) = \nabla \cdot \left(D_a \nabla n_e \right) + S_e \tag{1}$$

Mass continuity: $$\nabla \cdot (\rho v) = 0 \tag{2}$$

Momentum: $$\nabla \cdot (\rho v v) = -\nabla p + \nabla \tau \tag{3}$$

Electron energy: $$\nabla \cdot \left(\frac{5}{2} n_e k T_e v \right) = \left(v \cdot \nabla \right) p_e - \kappa_e \nabla T_e - Q_{elas} - Q_{rad} - Q_{ion} + \frac{j^2}{\sigma} \tag{4}$$

Ions and neutral species energy: $$\nabla \cdot \left(\frac{5}{2} n_h k T_h v \right) = \left(v \cdot \nabla \right) p_h - \kappa_h \nabla T_h + Q_{elas} \tag{5}$$

where n_e, n_h are the electron and the heavy particles densities, v is the velocity, D_a is the electron ambipolar diffusion coefficient, S_e is the electron source term with a single ionisation of argon, ρ is the plasma density, p, p_e and p_h are the total and the partially electron and heavy particles pressures respectively, τ is the stress tensor, k is the Boltzmann constant, κ_e and κ_h are the electron and heavy particles thermal conductivities, Q_{elas} is the energy exchange between electrons and heavy particles in elastic collisions, Q_{rad} is the radiation loss, Q_{ion} is the atoms ionization energy (or recombination energy), j^2/σ is the Joule effect with j the current density σ the electric conductivity. The balance equations are coupled to the state equation $p = (n_i + n_n)kT + n_e k T_e$ and the axial electric field E along the axis of the throat is $E = I / 2\pi \int_0^{r_c} \sigma r dr$ with a constant arc current I, where r_c is the radius of throat. The balance equations associated to the boundary conditions has been solved by the finite difference method developed by Patankar [10].

4. ARC VOLTAGE AND ELECTRIC POWER

One of the important performances of the arc-jet thruster is the electric power which is calculated from the value of the plasma conductivity at determined value of total arc current. For a long arc, in which arc column region dominates the calculation of arc tension is relatively easy because the electric field is constant. The arc voltage is determined by multiplying the electric field and the arc length. Experimental studies show that if the electric arc is formed in such conditions, that

the arc column with a conductive core can expand freely, while the current increases the arc voltage decreases. This is due to the fact that the increase in current results in the arc column cross-section increases and consequently the resistance and arc voltage decrease. If the electric arc is formed in a narrow channel, which prevents free enlarging of arc column diameter, while arc current increases, the current density and power transferred into the channel wall increase too. The energy balance shows that the increased power losses must be compensated by an increase in the power supplied to the arc, and therefore at constant current the arc voltage increases. In such conditions, the arc voltage-current characteristic is growing.

In the modeled arc-jet, electric arc is formed in a cylindrical channel with a length of 4 mm, so it is a short arc in which a voltage is determined by processes in the cathode flow region. In this region, the current passes by variable cross-section of conductive core of the arc. The smallest cross section occurs near the cathode. The value of this section results from the current density, which depends on the cathode material and for tungsten cathode can be taken about $2 \cdot 10^8$ A/m^2. Given value of density is the highest value, because as moving away from the cathode the cross-section increases, and thus the current density decreases.

In order to calculate the properties of plasma, the total arc current value is introduces into the numerical code, while in the energy equation the Joule energy per unit volume as a source term occurs which is proportional to the square of current density. It follows that the calculations must be verified using other measurable parameter, which may be a voltage or power supplied to the arc. In order to develop a method of the arc voltage determination the analysis of voltage-current characteristics obtained experimentally for various gas flow rates [11] has been carried out. These characteristics are shown in figure 2, while experimental values are indicated as points. The voltage-current characteristics are decreasing, and it can indicate that the arc voltage decreasing results from conductivity change with a current increasing.

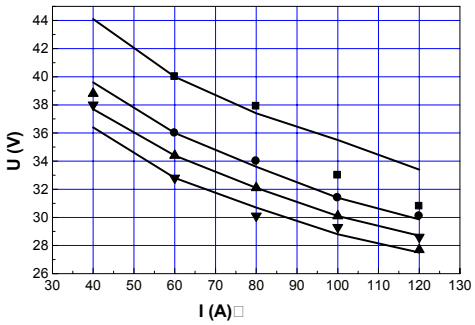

Fig. 2 – Voltage-current characteristics for argon flow rate of —■— 0.65 g/s, —●— 0.87 g/s, —▲— 1.075 g/s, —▼— 1.29 g/s (experimental data from [11] and model).

Electron and heavy particles temperatures and electron density are numerically determined for argon mass flow rate of 1.075 g/s (25 slm – standard liter per minutes) and arc current corresponding to experimental data. The increase in the arc current leads to increase of the temperatures (figure 3.a and 3.b), and the electron density (figure 3.c) in the arc, and thus the plasma conductivity. Using the calculated plasma parameters, the plasma conductivity is determined in the arc.

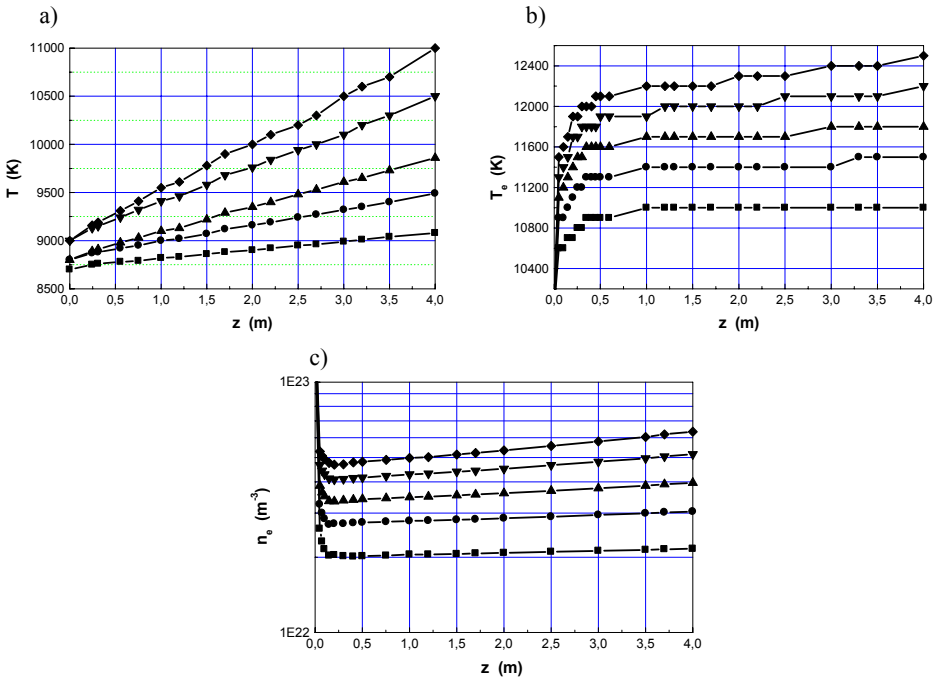

Fig. 3 – Distributions along the throat axis for argon flow rate of 1.075 g/s and a current of —■— 40 A, —●— 60 A, —▲— 80 A, —▼— 100 A, —♦— 120 A: a) heavy particles temperature, b) electron temperature, c) electron density.

Since the arc voltage is proportional to the resistivity, the axial distribution of $1/\sigma$ is presented for different currents (figure 4.a) showing that the curves are practically parallel to one another, and thus resistivity is inversely proportional to the arc current. Figure 4.b shows the value of $1/\sigma$ calculated on the axis, at the outlet of the throat as a function of arc current and for various gas flow rate. Comparing these distributions with the voltage-current characteristics a similar process could be seen. It implies that the average current density in the conductive core of cathode flow region is constant for different current values and constant gas flow rate. Using this assumption, the value of $\int_0^l \frac{1}{\sigma} dz$ is determined for conductivity taken on the axis of the plasma arc, where l is the length of the arc. For a fixed

value of current density and constant conductivity on cross section, there is the relationship $U = j \cdot \int_0^l \frac{1}{\sigma} dz$, so for one of the arc voltage value taken from experiment (in this case 60 A) the current density j is determined. Further, calculations are carried out by using such a fixed current density for different total current and calculating arc conductance on the basis of the numerical distributions of temperature and particles densities.

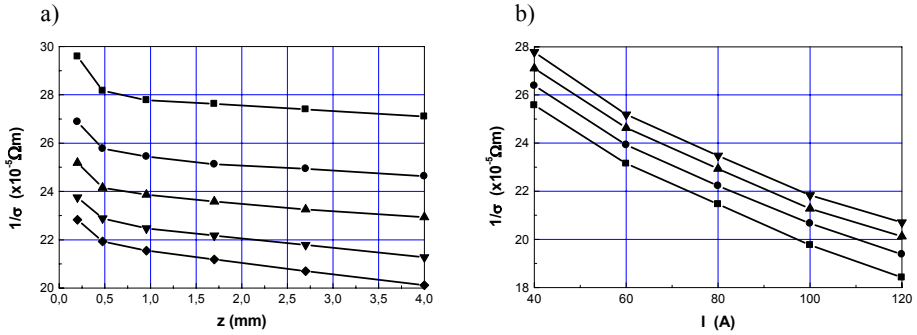

Fig. 4 – Plasma resistivity (1/σ) at the throat: a) for argon gas flow rate of 1.075 g/s and a current of —■— 40 A, —●— 60 A, —▲— 80 A, —▼— 100 A, —♦— 120 A, b) for argon gas flow rate of —■— 0.65 g/s, —●— 0.87 g/s, —▲— 1.075 g/s, —▼— 1.29 g/s.

Then, using the above relationship, the arc voltage as a function of current is determined. Calculated in such a way the voltage-current characteristics are shown in figure 2 as solid lines. The figure shows a good agreement between calculation and experimental results. This means that the current density in the cathode flow region could be taken as constant for different arc current values. The value of current density determined in such a way is the excessive because the value of the arc voltage measured experimentally contain cathode and anode voltage drop. However, these voltage drops can be easily incorporated into the calculations and the current density can be corrected.

The determination of the arc voltage curve, presented above, which uses the value of conductivity at the arc axis, is the approximate relationship, because the plasma conductivity changes in cross-section area. Therefore, in the accurate calculation the formula $U = \int_0^l \int_0^{r_c} \frac{I}{2\pi r \sigma} dr dz$ is used which incorporates the radial distribution of conductivity σ. It should be noted that the arc conductance is practically determined by the conductance in the center of the arc where it has a large, approximately constant value. The voltage-current characteristics for different values of the gas flow rates (figure 2) show that with the increase in the gas flow rates the arc voltage decreases. It is, therefore, the opposite behavior than that well known for a long arc. Experimental studies carried out in a wide range of

gas rates [11] confirm this dependence. In order to explain this dependence the electron and heavy particles temperature and density are analyzed.

Figure 5 shows that the calculated temperature of electrons and heavy particles decreases with the gas flow rate increasing which means a stronger cooling of the arc by the cold gas. The distribution of electron density (figure 6.a) shows that this density near the cathode is smaller for a smaller gas flow rate, while moving away from the cathode, this relationship turns and greater density is observed for a greater gas flow rate. The current density is determined based on a calculation of conductivity and arc voltage measured for one value of current.

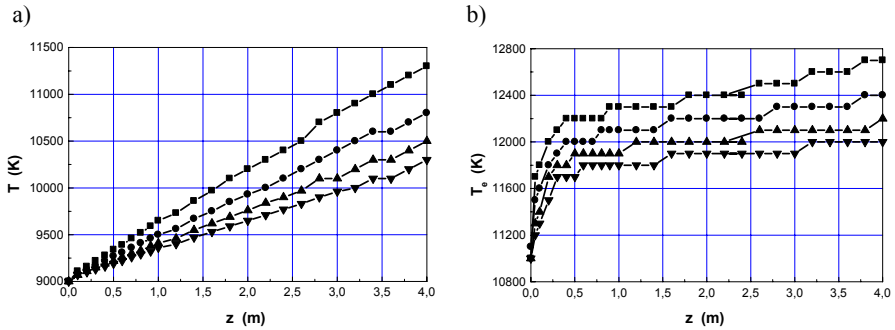

Fig. 5 – Axial distributions at the throat for arc current of 80 A and argon gas flow rate of —■— 0.65 g/s, —●— 0.87 g/s, —▲— 1.075 g/s, —▼— 1.29 g/s: a) heavy particles temperature, b) electron temperature.

Using the voltage-current characteristics the electric arc power is calculated and the greater gas flow rate, the smaller the arc power (figure 6.b). This is a very interesting result, because it means that in terms of efficiency of plasma thruster, it is advantageous to use high gas flow rate.

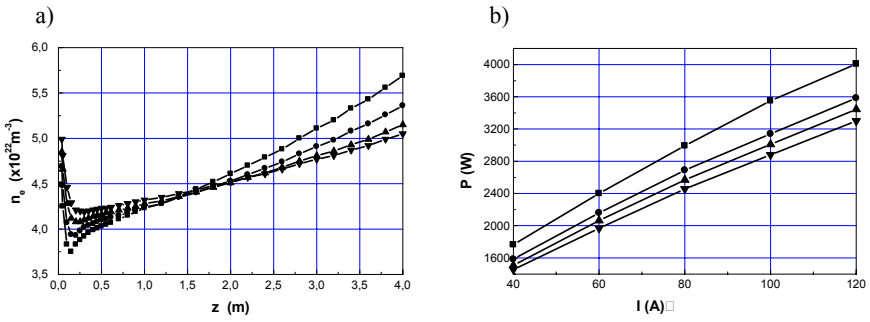

Fig. 6 – Distributions for argon flow rate of —■— 0.65 g/s, —●— 0.87 g/s, —▲— 1.075 g/s, —▼— 1.29 g/s: a) axial distributions of the electron density in the throat for an arc current of 80 A, b) electric input power as a function of the arc current.

5. THRUST, SPECIFIC IMPULSE AND EFFICIENCY

For the space applications of arc-jet as electric thruster, three parameters associated to the performances have to be determined and compared to the required performances for a chosen space mission. The first one is the axial thrust, the second one is the specific impulse correlated to the mass consumption for a given variation of velocity of the spacecraft and the last one is the global efficiency. The axial thrust F is deduced from the profiles of density and axial velocity and given by $F = \int_0^R \rho u_z^2 2\pi r\, dr$ where u_z is the axial component of velocity, r the radius and R the radius of nozzle exit section. The figure 7.a presents the axial thrust for three values of the ratio of the nozzle outlet and inlet sections A_2/A_1 *i.e.* 49, 100 and 210, given respectively the radius R_2 = 14 mm, 20 mm, 29 mm, at constant mass flow rate of 0.8 g/s and an arc current varying from 40 A to 120 A. This figure shows that for higher current the thrust rises of about 30% for a fixed A_2/A_1. The increase in current causes an increase in velocity and simultaneously the temperature and plasma density at the outlet of the nozzle. Therefore, the power is a very important factor determined the value of the thrust. It should be noted, however, that the value of current affect the power supplied to the arc, and thus efficiency of arc-jet. The thrust as gas flow rate function for a constant arc current and for the different ratio of A_2/A_1 is shows in figure 7.b. These results indicate that the thrust increases with the gas flow rate from a value around 0.3 N for the gas flow 0.4 g/s to 2.5 N for 1.2 g/s with a quasi linear variation above 0.8 g/s. To maximize the axial thrust, we aim to increase the velocity at relatively high density of the plasma. Furthermore, since the integral is over the outlet section of the nozzle the thrust will be large if the distributions of velocity and density will be flat. The calculation shows that the greater the ratio of A_2/A_1 (higher angle of the nozzle) the product ρu_z^2 is quasi constant in most parts of the nozzle, so it seems that the use of larger cross-section of the nozzle outlet is better. On the other hand, the increase of the angle of nozzle results in velocity component decreasing in the direction of the axis z. The comparison of thrust calculation using axial velocity u_z and the projection of this value on axis z shows that the difference does not exceed 9%. The calculations take into account, however, the axial velocity component projected on z axis. We would expect that by increasing the surface of the nozzle outlet we get more thrust. However, as shown in figures 7, thrust only slightly depends on the ratio A_2/A_1. This is due to the increase surface A_2 increases velocity, but also reduces the plasma density and the effect of thrust changing is much smaller than might be expected.

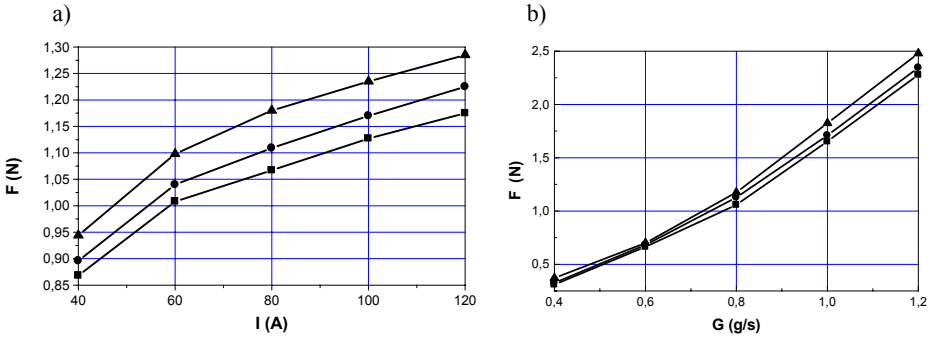

Fig. 7 – Thrust for the ratio A_2/A_1 of —■— 49, —●—100, —▲— 210: a) as function of arc current and at gas flow rate of 0.8 g/s, b) as function of gas flow rate and at arc current of 80 A.

The specific impulse I_{sp} is usually defined as $I_{sp} = \frac{F}{Gg_0}$ where G is mass flow rate and g_0 is the intensity of the gravity at the Earth ground level. The specific impulse is related to the gas velocity at the exit of the divergent part of the arc-jet and correlated to the mass consumption for a given variation of the spacecraft velocity.

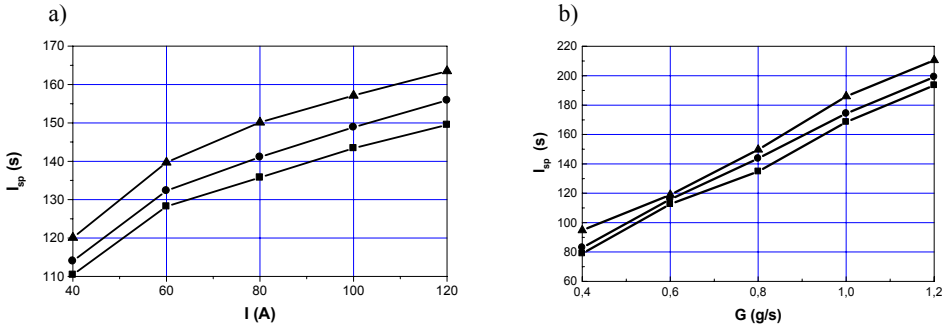

Fig. 8 – Specific impulse for the ratio A_2/A_1 of —■— 49, —●—100, —▲— 210: a) as a function of arc current and at a gas flow rate of 0.8 g/s, b) as a function of gas flow rate and at an arc current of 80 A.

A high specific impulse induces a low gas utilization and then a gain in mass of propellant. The specific impulse is varying from 80 to 210 s (figure 8.a and 8.b). At a fixed mass flow, the I_{sp} is proportional to the thrust F. The electric input power is varying from 1.5 kW to 4 kW. The global efficiency is defined by $\eta = \frac{F^2}{2G\left(Gc_{p0}T_0 + P\right)}$, where T_0 and c_{p0} are temperature and specific heat of inlet gas, P is the electric input power. In figure 9 the efficiency as arc current function

is shown, which demonstrates slightly increasing for current from 40 to 60 A, then decreasing with current. It should be noted, however, that for the currents from 40 to 120 A, these changes are relatively small, about 8% and results from the energy transfer to the wall of throat. Efficiency gains can also be obtained by increasing the outlet section of nozzle (figure 9). The calculation shows that for the gas flow rate 1.2 g/s achieved efficiency gains is about 10% when changing the ratio A_2/A_1 from 49 to 210.

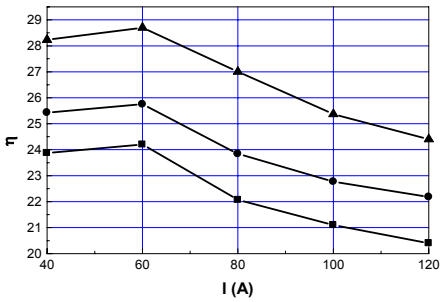

Fig. 9 – Efficiency as arc current function, at gas flow rate of 0.8 g/s and for the ratio A_2/A_1 of —■— 49, —●—100, —▲— 210.

The obtained values for the thrust and the specific impulse confirms the usual values for the application of arc-jet thruster (0.1N - 2N, 200s - 1500s) for many types of space missions. The high level of thrust is due to the mass flow rate and the low specific impulse to the low velocity at the nozzle exhaust. The specific impulse is lower than electric thruster one where charged particles are accelerated by an electromagnetic field.

6. CONCLUSION

A two-temperature fluid description allows to calculate the thermodynamical and hydrodynamical properties of a direct current (D.C.) arc-jet taking into account non equilibrium conditions for the ionization process and for the kinetic temperatures. The thrust, the specific impulse and the global efficiency are calculated for variation of the ratio between the cross sections at the nozzle outlet and inlet. For the studied conditions of mass flow rate and for the range of arc current (60-120 A), the calculated thrust is between 0.3 and 2.5 N, the specific impulse varies from 80 to 210 s and the arc jet efficiency from 20% to 30%. It has been shown that the thrust and the specific impulse increase with the arc current especially because of flow acceleration. However, for higher currents the energy loss to the wall becomes more and more important and the efficiency of arc-jet thruster diminishes. The study indicates that argon could be a cheap candidate for

arc-jet propulsion. The presented study allows concluding that design of arc-jet requires calculation permitting optimizing this kind of plasma sources. The developed numerical code is a very powerful tool for future developments of arc-jet thrusters with other atomic or molecular gases.

REFERENCES

1. L. E. Wallner, J. Jr. Czika, Arc-jet thruster for space propulsion, NASA TN D-2868, 1965.
2. E.Y. Choueiri, A Critical History of Electric Propulsion: The First Fifty Years (1906-1956) *J. of Propulsion and Power* 20 N°2 pp 193-203, 2004
3. M. Dudeck, F. Doveil, N. Arcis, S Zurbach, Plasma propulsion for geostationary satellites for telecommunication and interplanetary missions, 1st International Symposium on Electrical Arc and Thermal Plasmas in Africa (ISAPA), *IOP Publishing, IOP Conf. Series: Materials Science and Engineering* 29 (2012) 012010
4. Smart-1 European Space Agency BR-191 June 2002 and Smart-1: A Solar-Powered Visit to the Moon 2003 *ESA bulletin* Number 113, February 2003
5. C.R. Koppel, F. Marchandise, M. Prioul, E. Estublier, F. Darnon, The Smart-1 Electric Propulsion Subsystem around the Moon: In Flight Experience, 41th AUAA/ASME/SAE/ASEE Joint propulsion Conference, Tucson, Arizona 10-13 July 2005
6. M. Guyot, S. Denise, L. Dusseau, F. Saigné, M. Bernard, P. Claudé, M. Dudeck, Electrostatic propulsion for Satellites: Application to the Robusta-3 nanosatellite, *8th Conference of the French Society of Electrostatics*, Cherbourg-Octeville, France, 3-5 July, 2012, IEEE/TDEI, Vol. 21, Issue: 3, p.1161-1165, June 2014
7. S. Dandavino, C. Atamany , S. Chakraborty, H. Shea, C. Ryan, J. Stark, Design and fabrication of the thruster heads for the MicroThrust MEMS electrospray propulsion system, EPC-2013-127, *33rd International Electric Propulsion Conference*, Washington, D.C., USA, October 6-10, 2013
8. A. Kaminska, B. Lopez, B. Izrar, M. Dudeck, Modeling of an argon plasma jet generated by dc arc, *Plasma Sci. Technol*. 17 (2008) 035018 (12pp).
9. A. Kaminska, A. Bialek, M. Dudeck, Modeling of the plasma flow properties in a low power arc-jet, *Rom. J. Phys*. **59**, 745–756, 2014.
10. S.V. Patankar, *Numerical Heat transfer and Fluid Flow*, McGraw-Hill, New York, 1980.
11. V. Lago, A. Kaminska, M. Dudeck, Temperature, electron density and voltage-current characteristics, *Private communication*, Laboratoire d'Aérothermique du CNRS, Orléans, France 2007.